

Polymer and Silica Supported Tridentate Schiff Base Vanadium Catalysts for the Asymmetric Oxidation of Ethyl Mandelate – Activity, Stability and Recyclability

Rebecca A. Shiels,^a Krishnan Venkatasubbaiah,^a and Christopher W. Jones^{a,*}

^a School of Chemical & Biomolecular Engineering, Georgia Institute of Technology, 311 Ferst Drive NW, Atlanta, GA 30332, USA

Fax: (+1)-404-894-2866; phone: (+1)-404-385-1683; e-mail: cjones@chbe.gatech.edu

Received: August 4, 2008; Revised: October 22, 2008; Published online: November 19, 2008

Abstract: Homogeneous tridentate Schiff base vanadium catalysts derived from salicylaldehydes and *tert*-leucinol or *tert*-leucine are known to be excellent catalysts for the asymmetric oxidation of α -hydroxy esters including ethyl mandelate. Herein, new analogous supported, semi-soluble and insoluble catalysts are synthesized and their activities relative to the homogeneous catalyst are reported. The new catalysts are characterized by ¹H and ¹³C NMR spectroscopy, mass spectrometry (EI, ESI, FAB), X-ray crystallography, elemental analysis, gel permeation chromatography (GPC), Fourier transform infrared (FT-IR) spectroscopy, and nitrogen physisorption. The effects of support material, synthesis procedure, and reaction solvent are examined to probe the utility of these catalysts. Linear poly(styrene) supported catalysts are partially soluble under the reaction condi-

tions, and it is shown that the soluble species contribute significantly to the catalytic reactivity. Insoluble catalysts based on the same vanadyl complexes supported on cross-linked poly(styrene) resin or mesoporous silica allow for catalyst recovery and recycle, showing equivalent selectivities over multiple reaction cycles. The mesoporous silica supported catalyst exhibits greater selectivity than the analogous homogeneous and polymer supported catalysts. Rigorous recycle studies show a loss of activity in each recycle, which is attributed to the decomposition of some portion of the vanadyl complexes in each cycle.

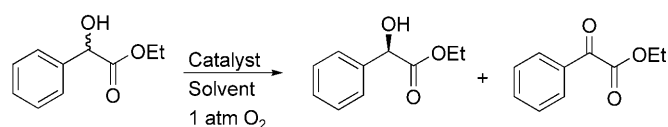
Keywords: immobilization; kinetic resolution; oxidation; polymer-supported catalyst; silica supported-catalyst

Introduction

The ability to synthesize enantiomerically pure α -hydroxy esters is of significant interest because these compounds are useful building blocks for chiral syntheses in the pharmaceutical and fine chemical industries.^[1] A great deal of research has been devoted to discovering catalytic systems that can efficiently generate enantiomerically pure α -hydroxy esters and other secondary alcohols,^[2–4] and an important subset of these systems exploit the kinetic resolution of racemic substrates through the appropriate selection of catalyst and reaction conditions.^[5–10] One such system that effectively utilizes kinetic resolution to yield enantiomerically pure alcohols from racemic mixtures involves the application of vanadium complexes with Schiff base ligands for selective oxidation with molecular oxygen. Specifically, tridentate Schiff base vanadium catalysts derived from salicylaldehydes and *tert*-leucinol or *tert*-leucine have been shown to promote the oxidative kinetic resolution of racemic α -hydroxy

esters by the selective oxidation of only one enantiomer (Scheme 1).^[11–13] This reaction is particularly attractive not only due to the high enantioselectivity it imparts but also due to the use of molecular oxygen at atmospheric pressure as the primary oxidant. Molecular oxygen is highly abundant, low in cost, and non-toxic, which make it more attractive than other oxidants, particularly inorganic oxidants that can be expensive and potentially hazardous to dispose of after use.

Previous research efforts in our group have investigated the immobilization of enantioselective homogeneous catalysts for improved catalyst performance,



Scheme 1. Oxidative kinetic resolution of an α -hydroxy ester.

with the key parameters by which performance is judged being productivity, selectivity, ease of recovery, and recyclability. This research predominantly focused on the immobilization of cobalt salen catalysts for application in the hydrolytic kinetic resolution (HKR) of epoxides, and a number of successful polymer supported catalysts have resulted from these efforts.^[14–16]

Since the tridentate Schiff base vanadium catalysts used in the oxidative kinetic resolution reaction resemble “half” salen functionalities, we set out to apply the knowledge gained from the immobilization of the cobalt salen HKR catalysts to the development of immobilized vanadium oxidative kinetic resolution catalysts. Even though the activities of the homogeneous catalysts are well-established, there are, to the best of our knowledge, no reports of analogous immobilized catalysts derived from salicylaldehydes and *tert*-leucinol for the oxidative resolution reaction. There are reports of supported manganese salen catalysts for the oxidative kinetic resolution of secondary alcohols, although these reports utilize diacetoxyiodobenzene as the oxidant instead of molecular oxygen.^[10,17,18] Also, in one case, the enantiomeric excesses reported were very low.^[17] Therefore, we sought to develop active and selective supported catalysts for this reaction that are straight-forward to synthesize and that utilize molecular oxygen instead of an organic oxidant. Since the removal of the residual metal from the product is important due to economic, environmental, and product quality issues, the ability to have a recoverable and recyclable catalyst that can be easily removed from the product mixture is very attractive. We report here our description of the immobilization of these vanadium catalysts on semi-soluble polymers, on insoluble polymers and on SBA-15 mesoporous silica, and we demonstrate their utility in the oxidative kinetic resolution of ethyl mandelate. Particular attention is paid to a rigorous study of catalyst recycle.

Results and Discussion

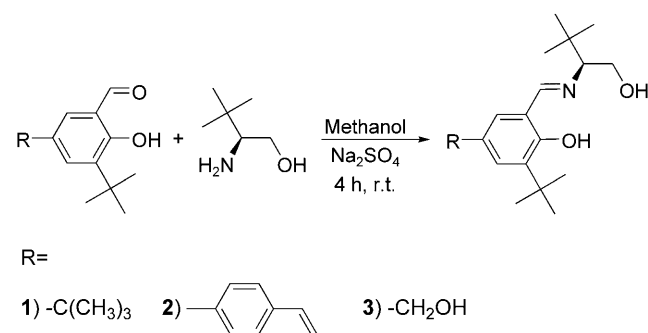
Polymer Catalyst Syntheses and Characterization (2a', 2b' and 2c')

In general, there are two strategies for developing immobilized polymer catalysts. The first strategy involves grafting the desired catalyst functionality onto an insoluble polymeric support such as a resin. This is an efficient way to create a heterogeneous catalyst, but if the procedure is performed in a step-wise manner or if the surface reaction is not quantitative, many types of species can exist on the resin surface. In order to circumvent this issue, a second strategy for immobilization is employed which involves the direct polymerization of monomers containing the de-

sired catalyst functionality. Since previous research in our group utilized the second method to synthesize polymeric salen catalysts for the hydrolytic kinetic resolution of epoxides with much success, we elected to use this approach first in this work.^[14–16]

The monomer bearing both the desired ligand functionality and a styryl group capable of being polymerized (**2**) was produced using a synthetic procedure similar to those reported in the literature (Scheme 2). The formation of **2** was confirmed by ¹H NMR, ¹³C NMR, mass spectrometry (ESI) and elemental analysis. To verify and prove the coordination mode of **2** with vanadium, we prepared the vanadyl complex of **2** (metalated-**2**) using vanadium oxytriisopropoxide [VO(O-*i*-Pr)₃]. Complex formation was confirmed by FAB mass spectrometry as well as single crystal X-ray crystallography. The molecular structure from X-ray crystallography revealed that the vanadium is in a pentacoordinated environment with a distorted tetragonal pyramid geometry. The V–O bond distances are comparable with literature precedents and decrease in the order of phenolate oxygen [1.895(5) Å], alcoholato oxygen [1.839(6) Å], ethanolato oxygen [1.756(6) Å] and V=O oxygen [1.602(6) Å].^[19] The V1–N1 distance is 2.079(5) Å, which is well within the range of reported literature values of similar complexes. The ORTEP diagram and metric parameters of metalated-**2** are given in Figure 1.

Linear polymers of **2** were prepared by the AIBN initiated free radical homopolymerization of the styryl monomer (**2a**) or copolymerization of the styryl monomer with styrene (**2b**) (Scheme 3). ¹H NMR spectroscopy of the polymers exhibited the typical broadening features that are expected for macromolecules (Figure 2). Also, the peaks associated with the vinyl protons in the monomer spectrum ($\delta = 5.0–6.0$) were absent in the polymer spectra, which indicated that residual monomer was removed during the isolation of the polymers. Using gel-permeation chromatography (GPC) in THF with poly(styrene) standards, the number average molecular weight (M_n) of the homopolymer was determined to be 5,330 with a polydispersity index (PDI) of 2.16. This corresponds to an



Scheme 2. Synthesis procedure for catalyst ligands.

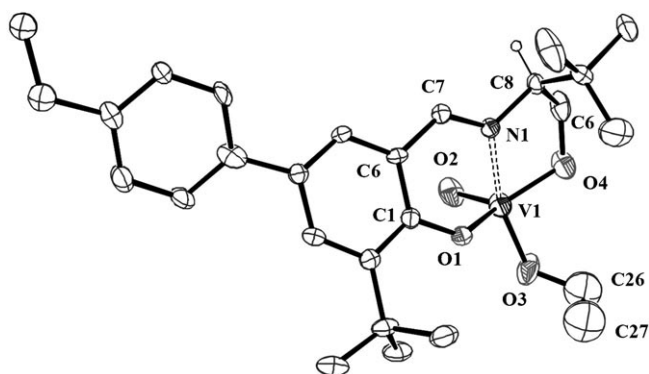


Figure 1. Molecular structure of metalated **2** with thermal ellipsoids at the 30% probability level. Hydrogen atoms except the one attached to C8 are omitted for clarity. Selected interatomic distances (Å) and angles (°): distances V1–O1 1.895(5), V1–O2 1.602(6), V1–O3 1.756(6), V1–O4 1.839(6), V1–N1 2.079(5); angles O1–V1–O4 140.9(3), O2–V1–O4 108.6(3), O2–V1–O3 103.9(3), O3–V1–N1 160.1(3)

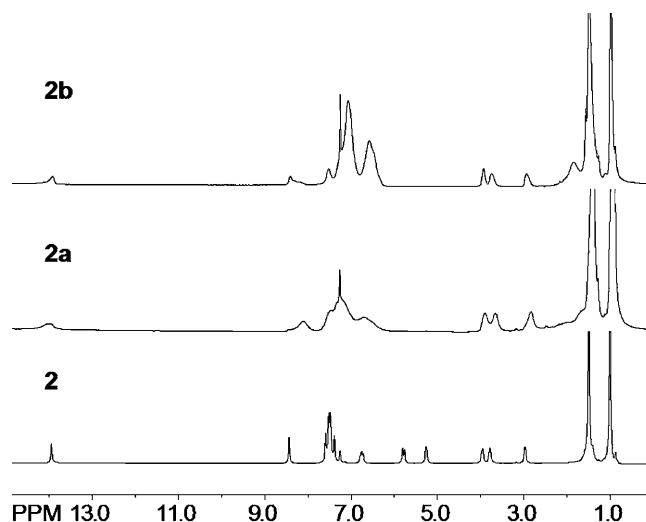
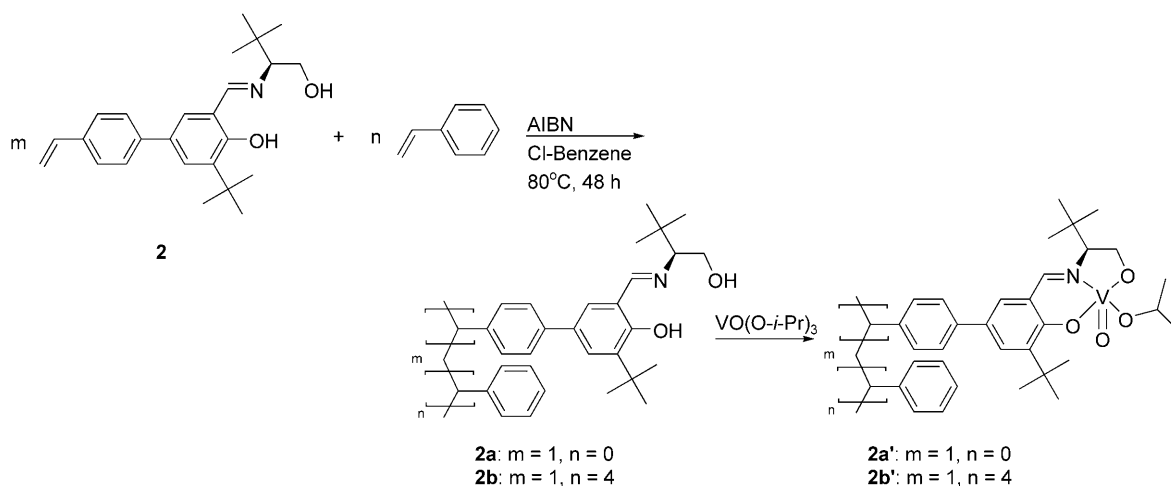


Figure 2. ^1H NMR spectra of styryl functionalized monomer **2**, homopolymer **2a**, and copolymer **2b**.

average of 14 repeat units in the polymer chain. The M_n of the copolymer was determined to be 8,439 with a PDI of 2.01. This corresponds to an average of 11 catalyst repeat units with a 2:5 ligand to styrene ratio (determined from ^1H NMR). These data are summarized in Table 1.

The homo- and copolymers were metalated using $\text{VO}(\text{O-}i\text{-Pr})_3$ to form catalysts **2a'** and **2b'**. The vanadium content of the metalated polymers was determined by elemental analysis. In the case of homopolymer **2a'**, the vanadium loading was 10.3 wt% (2.02 mmol/g), which corresponds to roughly 87% of the Schiff base ligand being metalated. For copolymer **2b'**, the vanadium loading was 6.0 wt% (1.18 mmol/g), which corresponds to roughly 83% of the Schiff base ligand being metalated.

The metalated polymers were characterized by Fourier transform infrared spectroscopy (FT-IR) (Figure 3). The spectra for homopolymer **2a'** and copolymer **2b'** closely resemble one another, and both exhibit the expected peaks that indicate the presence of the immobilized catalyst functionality (Table 2). Particularly noteworthy is the strong $\text{C}=\text{N}$ stretch located at 1617 cm^{-1} which is indicative of the coordination of the imine nitrogen with the vanadium. This stretch would be expected to appear around 1630 cm^{-1} if the ligand was not coordinated with the vanadium.^[20] Also, the $\text{V}=\text{O}$ stretch is seen at 986 cm^{-1} in the homopolymer and 984 cm^{-1} in the copolymer, and these values are in line with reported literature values.^[13,19–21]



Scheme 3. Synthesis of linear poly(styrene) catalysts **2a'** and **2b'**.

Table 1. Polymeric ligand characterization.

Polymer	Mn ^[a]	PDI ^[a]	m,n actual ^[b]
2a	5,330	2.16	14, 0
2b	8,439	2.01	11, 28

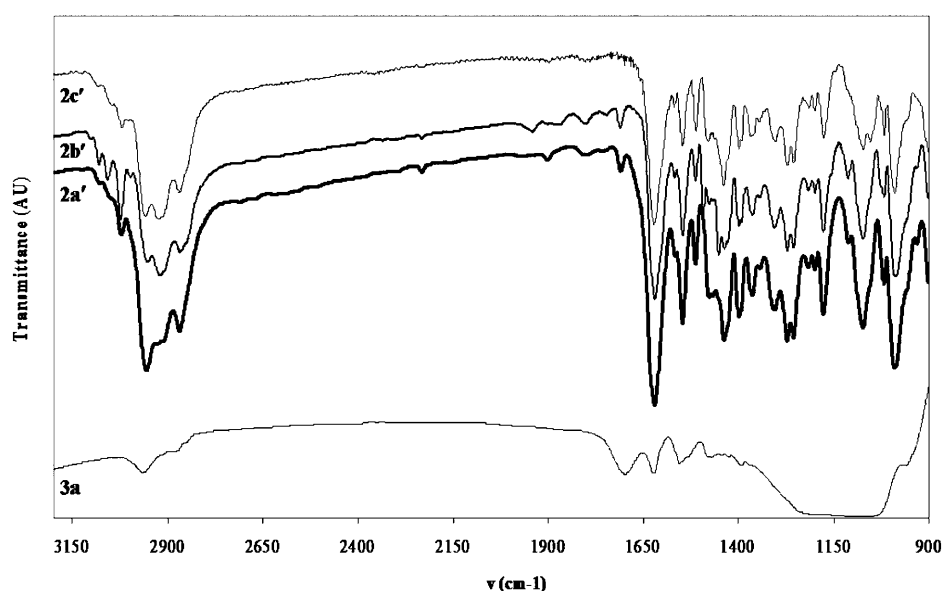
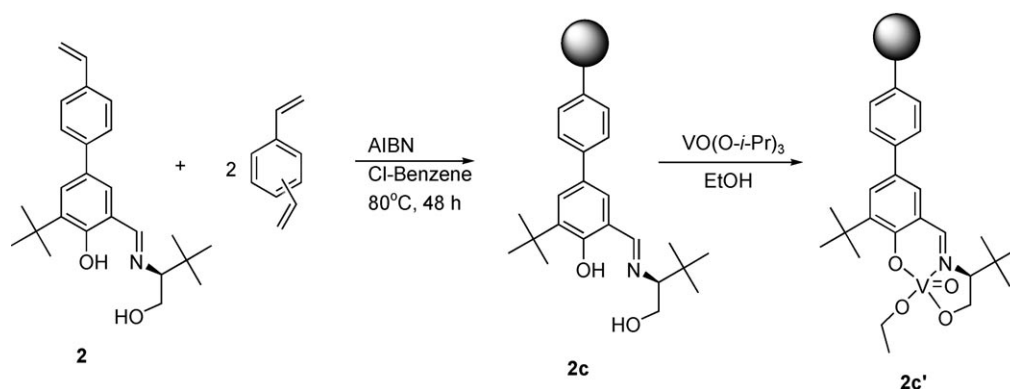
^[a] From GPC in THF with poly(styrene) standards.

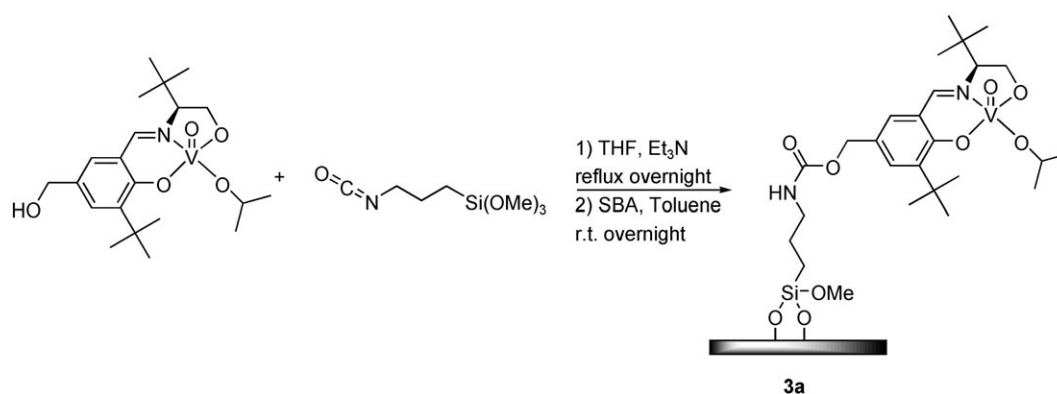
^[b] Calculated from Mn and ¹H NMR; m=repeat units of catalyst ligand, n=repeat units of styrene.

Cross-linked polymer **2c** was prepared by the copolymerization of **2** and divinylbenzene (Scheme 4). Metalation of **2c** with VO(O-*i*-Pr)₃ in ethanol at 60 °C produced the resin catalyst **2c'**. Elemental analysis indicated a vanadium loading of 5.3 wt% (1.04 mmol/g), which corresponds to roughly 68% of the Schiff base ligand being metalated. The FT-IR spectrum of **2c'** shows a strong C=N stretch at 1620 cm⁻¹, indicating that the vanadium is coordinated with the imine nitrogen, and a V=O stretch at 987 cm⁻¹, which is consis-

Table 2. FT-IR data (KBr disk) for metalated polymeric catalysts **2a'**, **2b'**, **2c'**, and silica catalyst **3a**.

	2a' ν [cm ⁻¹]	2b' ν [cm ⁻¹]	2c' ν [cm ⁻¹]	3a ν [cm ⁻¹]
C–H aromatic and aliphatic stretches	3020, 2953, 2908, 2867	3055, 3021, 2948, 2908, 2862	3017, 2955, 2914, 2865	2956, 2871, 2845
C=N	1617	1617	1620	1617
V=O	986	984	987	955

**Figure 3.** FT-IR spectra of resin catalyst **2c'**, copolymer catalyst **2b'**, homopolymer catalyst **2a'**, and silica catalyst **3a****Scheme 4.** Synthesis of cross-linked resin catalyst **2c'**.



Scheme 5. Synthesis of silica supported vanadium Schiff base catalyst **3a**.

tent with our results above for the other polymer catalysts.

Silica Supported Catalyst Synthesis and Characterization (**3a**)

A trialkoxysilane functionalized catalyst analogue was synthesized as described in the Experimental Section (Scheme 5). This analogue was then grafted onto SBA-15 silica, and the resulting supported catalyst **3a** was characterized. FT-IR was used to determine the nature of the organic species on the silica surface (Figure 3). The spectrum shows the anticipated peaks which suggest that the catalyst functionality is supported on the silica surface (Table 2). Of particular interest are the C=N stretch at 1617 cm^{-1} , indicating the vanadium is coordinated with the imine nitrogen, and the V=O stretch at 955 cm^{-1} . These values are in line with those reported for similar materials.^[20]

Nitrogen physisorption provided additional evidence that the catalyst was immobilized in the mesopores of the silica. The SBA-15 prior to functionalization as well as after functionalization exhibits a type IV isotherm with hysteresis, which is indicative of its mesoporous nature. The bare SBA-15 had a BJH average adsorption pore diameter of 65 \AA , whereas the vanadium functionalized material had a BJH average adsorption pore diameter of 62 \AA . Also, the BET surface area for the SBA-15 silica material decreased from $858\text{ m}^2/\text{g}$ before functionalization to $325\text{ m}^2/\text{g}$ after functionalization. This is typical of what is observed when grafted organometallic or organic species block access to the micropores that are known to exist in many samples of SBA-15, and thus much or all of the microporous surface area is no longer included in the total surface area calculation.^[22–25]

Oxidative Kinetic Resolution using Metalated-1 as Catalyst

To provide a benchmark for our supported catalysts, we conducted experiments with both the homogeneous catalyst (metalated-1) and unligated $\text{VO}(\text{O}-i\text{-Pr})_3$ to determine their reactivities toward the oxidation of ethyl mandelate. The reactivity of metalated-1 was tested in dry acetone, dry acetonitrile, and dry dichloromethane as described in the Experimental Section for Method 1. The results showed acetone to be the best solvent for the reaction, providing $>99\%$ conversion of *S*-ethyl mandelate and 99% enantiomeric excess (*ee*) of *R*-ethyl mandelate in less than 4 h (Figure 4) (total conversion *S*+*R*: 54%). Acetonitrile was also a suitable solvent, providing $>99\%$ conversion of *S*-ethyl mandelate and 99% *ee* of *R*-ethyl mandelate in 5 h (total conversion *S*+*R*: 50%). However, the resolution was significantly slower in dichloromethane, reaching only 85% conversion of *S*-ethyl mandelate and 79% *ee* of *R*-ethyl mandelate after 7 h. This trend is similar to that reported by Toste, although the reaction times found in this report are different than those for their system.^[11]

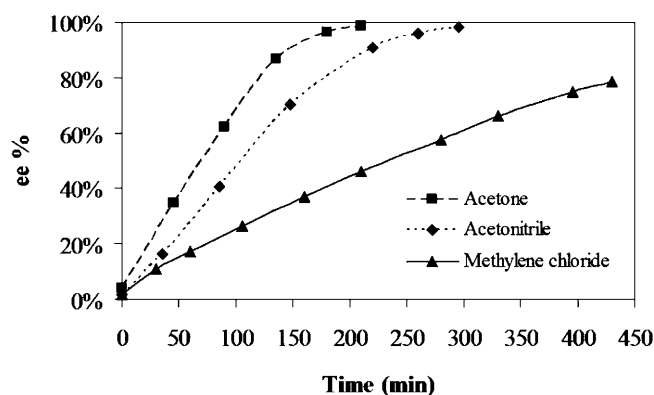


Figure 4. Enantiomeric excess of *R*-ethyl mandelate vs. time for homogeneous catalyst **1** in various solvents.

Since the homogeneous catalyst (metalated-**1**) is metalated *in situ* prior to reaction, the catalytic activity of VO(O-*i*-Pr)₃ alone was probed to determine if this compound plays a part in the oxidation of ethyl mandelate if it is not fully ligated by the Schiff base ligand. Test reactions were conducted in both dry acetone and dry acetonitrile and were allowed to run for 23 h. At the end of this period, the reaction in acetone yielded a total ethyl mandelate conversion of only 7% with no increase in *ee*. The reaction in acetonitrile gave a total ethyl mandelate conversion of 5% with no increase in *ee*. These results suggest that any catalytic contribution from free VO(O-*i*-Pr)₃ in solution can be neglected relative to the contribution from the metalated ligand.

Oxidative Kinetic Resolution using Polymeric Catalysts **2a'** and **2b'**

Since acetone was the most effective solvent for the oxidative kinetic resolution of ethyl mandelate with the homogeneous catalyst, all reactions using the polymeric catalysts were conducted in acetone. To investigate the activity of the homo- and copolymers, two catalyst metalation methods were employed: *in situ* metalation (Method 1) and metalation and isolation prior to reaction (Method 2).

First, homopolymer catalyst **2a'** was assessed using Method 1 and Method 2. Significant differences in reaction rates were observed between the two catalyst metalation methods (Figure 5). The homopolymer catalyst that was metalated and isolated prior to use (Method 2) was significantly less active than the homopolymer catalyst that was metalated *in situ* (Method 1). For instance, after 9 h of reaction, the Method 1 reaction had proceeded to 94% conversion of *S*-ethyl mandelate and 88% *ee* of *R*-ethyl mandelate, whereas the Method 2 reaction had only reached

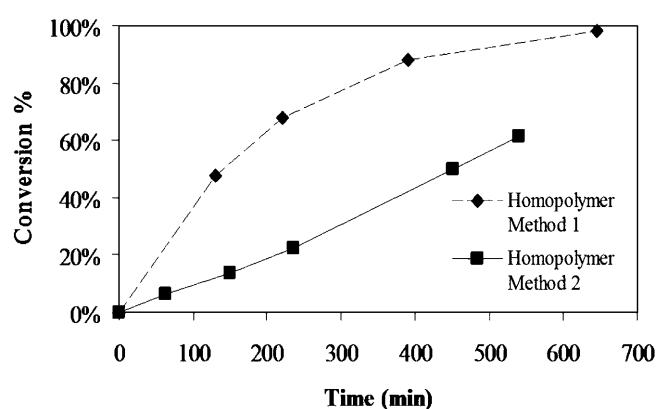


Figure 5. Conversion of *S*-ethyl mandelate vs. time for homopolymer catalyst **2a** with *in situ* metalation (Method 1) and metalation and isolation (Method 2).

61% conversion of *S*-ethyl mandelate and 42% *ee* of *R*-ethyl mandelate. We attribute this behavior to the higher solubility of the *in situ* metalated catalyst compared to the catalyst prepared *via* metalation and isolation. Specifically, after addition of VO(O-*i*-Pr)₃ to the solution of ligand **2a** dissolved in acetone, the products remained fully soluble initially, and no solid precipitation was observed for approximately the first hour of the reaction. After that time, some solid polymeric material began to precipitate from solution. However, when the premetalated complex, **2a'**, was added to acetone, solid polymeric material was always observed in the reaction flask, and complete dissolution was never achieved.

Copolymer catalyst **2b'** was also studied in the oxidative kinetic resolution of ethyl mandelate. Method 1 (*in situ* metalation) was examined first. In this case, it was observed that a portion of metalated polymer precipitated out of solution during the initial oxygen pre-treatment prior to reaction. Also, as the polymer precipitated, it formed large agglomerates which broke into smaller particles as the reaction proceeded. Nonetheless, copolymer catalyst **2b'** successfully completed the resolution, taking 9.5 h to reach 99% conversion of *S*-ethyl mandelate with 98% *ee* of *R*-ethyl mandelate (total conversion *S*+*R*: 58%) (Figure 6).

When Method 2 (metalation and isolation) was used with copolymer catalyst **2b'**, the catalyst was able to reach 99% conversion of *S*-ethyl mandelate and 95% *ee* of *R*-ethyl mandelate in 8 h (total conversion *S*+*R*: 61%), even though complete dissolution of the polymeric material was not observed. This copolymer catalyst gives roughly comparable reaction rates regardless of metalation method.

Since these catalysts were not fully soluble in the reaction media, we sought to assess whether the active species were associated with soluble polymeric species or precipitated polymer species. To probe this,

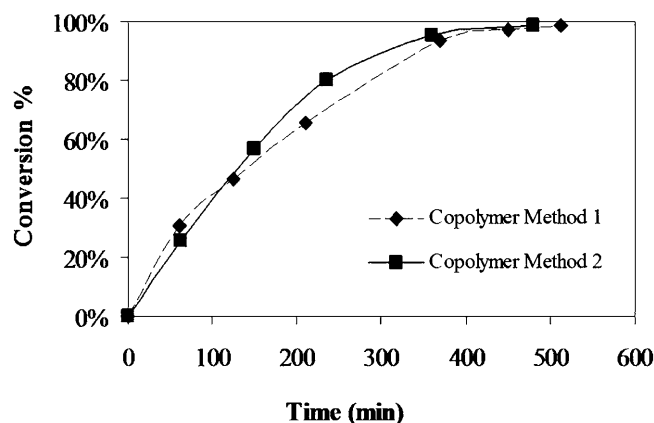


Figure 6. Conversion of *S*-ethyl mandelate vs. time for copolymer catalyst **2b** with *in situ* metalation (Method 1) and metalation and isolation (Method 2).

Table 3. Reaction rate data for catalysts **1**, **2a'**, **2b'**, **2c'** and **3a**.

Catalyst	Metalation Method	Solvent	Initial Rate ^[a]	Time [h]	Total Conversion [%]	ee [%]	s ^[b]
1	1	acetone	5.7	3.5	54	98	50
1	1	acetonitrile	3.9	5	50	98	458
1	1	dichloromethane	2.0	6	48	71	16
2a'	1	acetone	2.1	10.75	57	96	24
2a'	2	acetone	0.6	9	35	42	12
2b'	1	acetone	3.1	9	58	97	23
2b'	2	acetone	2.5	8	61	97	17
2c'	2	acetone	1.8 ^[c]	10.5	63	95	12
2c'	2	acetone	1.2 ^[d]	10.5	48	68	13
3a	2	acetone	1.3	11	48	96	204
3a	2	acetonitrile	1.3	11	49	93	211

^[a] mol *S*-ethyl mandelate/(mol V hour).

^[b] $s = [\ln(1 - \text{conv.})(1 - ee)] / [\ln(1 - \text{conv.})(1 + ee)]$.

^[c] First cycle.

^[d] Fourth cycle

copolymer **2b'** was metalated using Method 1 and used in a series of reactions. After complete conversion of the *S*-ethyl mandelate in reaction 1, the solid polymer was removed *via* filtration and a fresh batch of reactants was added to the filtrate and monitored for additional reaction. The reaction in the second, solid-free reaction proceeded at a rate similar to but slightly less than the first reaction, suggesting the reactivity from the first reaction is associated with, at least in part, soluble polymer catalyst.

The initial rates and selectivity factors for the catalysts are tabulated in Table 3. We note that all the rates differ by less than a factor of 10. Furthermore, the selectivity factors for the polymer immobilized catalysts (**2a'**, **2b'**, **2c'**) are similar to the those of the parent homogeneous catalyst, **1**, in acetone. Surprisingly, the selectivity factor for the catalyst supported on mesoporous silica (**3a**) was significantly higher, suggesting that the nature of the support (or linker) can play an important role in the catalyst selectivity.

To probe the scope of the catalyst **2c'** in asymmetric oxidation, reactions were performed with four additional substrates. The results are presented in Table 4. The alkyl substrate (entry 4) resolved with good selectivity followed by substrates bearing α -phenyls. Within the substrates bearing α -phenyls, the benzyl-substituted species (entry 3) resolved better than the ethyl and methyl derivatives.

To assess whether oxygen solubility in the liquid media might limit the initial rates, two experiments were run using metalated-**1** as catalyst with different oxygen pressures. After 60 min, the conversion running under standard conditions with the reaction head-space purged with pure oxygen was comparable to the conversion when running under 45 psig of oxygen pressure (~51 vs. 57%), suggesting that oxygen solubility is not a dominating rate-controlling step under the standard reaction conditions.

Table 4. Kinetic resolution of α -hydroxy esters.

Entry	R ¹	R ²	Time [h]	Conversion ^[a] [%]	ee ^[a] [%]	s ^[b]
1	Ph	OEt	10.5	63	95	12
2	Ph	OMe	9	52	77	14
3	Ph	OCH ₂ Ph	18	56	91	19
4	Me ₂ CH	OCHMe ₂	87	54	90	23

^[a] Determined by chiral GC or chiral HPLC.

^[b] $s = [\ln(1 - \text{conv.})(1 - ee)] / [\ln(1 - \text{conv.})(1 + ee)]$.

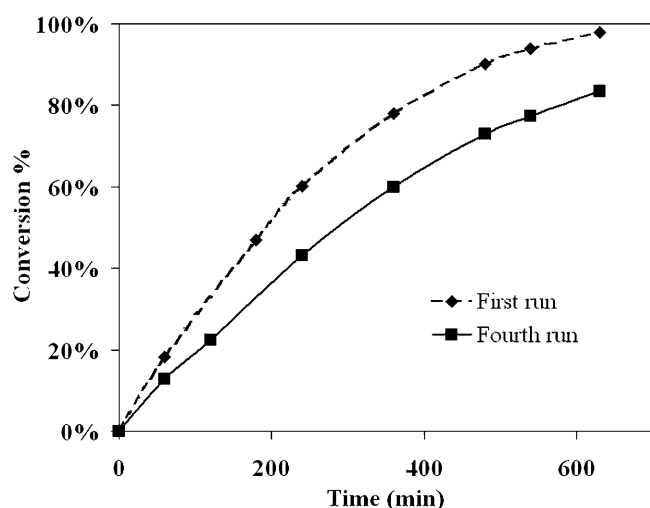
Oxidative Kinetic Resolution and Recycling Studies using Catalysts **2c'** and **3a**

Solid, completely insoluble catalysts were evaluated in these reactions in an effort to develop easily recyclable systems. First, the cross-linked resin catalyst **2c'** was evaluated for the kinetic resolution of ethyl mandelate. In comparison with the semi-soluble homo- and copolymers **2a'** and **2b'**, the insoluble resin **2c'** gave a similar reaction rate. For instance, copolymer **2b'** reaches 99% conversion of *S*-ethyl mandelate in 9 h, whereas the resin **2c'** converts 94% of the *S* enantiomer in the same duration. Silica catalyst **3a** was also tested in the oxidative kinetic resolution of ethyl mandelate in both dry acetone and dry acetonitrile. For the reaction in acetone, the resolution was complete in 11 h, reaching 99% conversion of *S*-ethyl mandelate and 98% ee of *R*-ethyl mandelate (total conversion *S*+*R*: 49%). The reaction in acetonitrile proceeded at the same rate, also taking 11 h to complete the resolution.

Table 5. Recycle data for the oxidation of ethyl mandelate with catalyst **2c'** after 16 h.

Cycle	Loading (mol%)	Conversion of <i>S</i> -ethyl mandelate [%]	<i>ee</i> [%] of <i>R</i> -ethyl mandelate
1	5.5	99	96
2	5.5	99	96
3	5.5	> 99	> 99
4	5.5	> 99	> 99

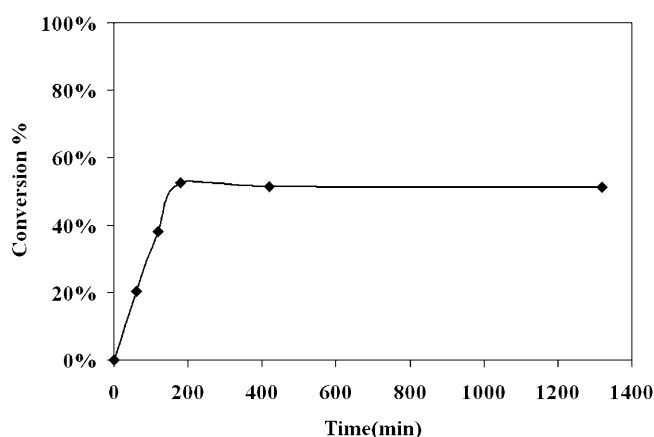
Recycling experiments were done using the insoluble catalysts **2c'** and **3a** by recovering the catalysts, washing, and reusing them in subsequent reactions with fresh reagents. The conversion of *S*-ethyl mandelate after 16 h was 99% using **2c'** over four cycles (Table 5). We note that standard practice in the literature describing supported catalysts would suggest a conclusion of “catalysts can be recycled without loss of activity” would be reasonable. However, this would be an improper conclusion, as it is based on measuring reaction yields at long times. In contrast, measurements of the reaction kinetics clearly suggest there is a gradual decrease in reaction rate upon recycle. A comparison of the kinetic profiles of the *S* enantiomer conversion in the first and fourth reaction cycles using catalyst **2c'** is given in Figure 7. After 10.5 h, the conversion in the first cycle was 98% of the *S* enantiomer, whereas the conversion was only 83% after the same time in the fourth cycle. The initial rate calculated for the first reaction cycle was 1.8 h^{-1} , whereas the initial rate calculated for the fourth reaction cycle was 1.2 h^{-1} . These results clearly suggest that there is a decrease in activity with each cycle even though the final conversions are similar at long times. To probe the reason for the decrease in activity, we compared

**Figure 7.** Recycle experiments for the conversion of *S*-ethyl mandelate vs. time with catalyst **2c'**, comparison of the first and fourth reaction cycle.

the elemental analysis of the fresh catalyst **2c'** and the used catalyst after the fourth cycle. Elemental analysis indicated a 50% loss in nitrogen and vanadium but only a 1% loss in carbon. From these results we hypothesize that imine cleavage leads to the loss of vanadium which results in decreased catalyst activity. It should be noted that a similar mode of deactivation of supported salen catalysts was also suggested in our recent work on the hydrolytic kinetic resolution of epoxides.^[26] Filtration tests using the catalyst **2c'** suggest that the reaction does not proceed in the absence of the solid catalyst (Figure 8).^[27]

We also performed recycling experiments using silica supported catalyst **3a**. In this case, a gradual decrease in activity in each cycle was again observed. Elemental analysis of the catalyst after the third cycle showed a decrease in the nitrogen and carbon percentages but surprisingly, no decrease in the vanadium loading. We propose that after complex degradation due to imine cleavage (or other mechanisms) the released vanadyl ions may be captured by the silica support. This would explain the observed loss of activity without loss of vanadium from the silica catalyst and is consistent with the known stability of vanadia/silica materials.^[28,29] To support this possibility, we stirred SBA-15 with vanadium oxytriisopropoxide in acetone for 18 h, filtered the solid material, washed it with acetone, and dried it under vacuum. The vanadium content (1.65 mmol/g or >65% of the added vanadium) of this material suggested that SBA-15 will effectively capture leached vanadyl ions from decomposed complexes.

We note that it is quite uncommon for researchers to study recyclability of supported coordination complex catalysts in the manner described in this section. Rigorously analyzing for catalyst decomposition and studying kinetics upon recycle is not routinely practiced. Rather, many researchers simply recycle catalysts and measure yields only at very long times. Such

**Figure 8.** Filtration test using catalyst **2c'**: the reaction was filtered after 3 h to probe the heterogeneity of the reaction.

an approach effectively hides complex deactivation and leads to the false conclusion that the catalysts are fully stable and recyclable. The decomposition of the imine-containing ligand here and in our related work on Co-salen catalysts suggest that the instability of ligands that contain this imine functional group may limit the number of recycles that can be achieved in many cases.

On the Mechanism of the Oxidative Kinetic Resolution

In our previous work on supported Co-salen catalysts for the hydrolytic kinetic resolution of epoxides, the reaction rates could be substantially enhanced over the rate using the parent small molecule complex by using properly designed supported catalysts. This is due to the importance of a hypothesized cooperative bimetallic slow step in the catalytic cycle, whereby two Co-salen complexes simultaneously interact with the epoxide reactant. As Toste and Chen have both hypothesized a mechanism for the oxidative kinetic resolution of α -hydroxy esters that includes a step where two vanadium complexes interact, we sought to see if there was any influence of catalyst structure on rate.^[11,12] The initial rate data in Table 3 suggest that all the catalysts studied here, including the parent small molecule complex, the semi-soluble polymers and the insoluble solid catalysts all catalyze the reaction with roughly similar rates. In addition, no enhancement in rates is seen using the supported catalysts (which force catalytic sites to be in close proximity) compared to the small molecule, parent complex at lower catalyst loadings. Hence, in this work there appears to be no evidence for the presence of a bimetallic step that is kinetically significant in this reaction, although this does not preclude the occurrence of a kinetically insignificant bimetallic step.

Conclusions

We have developed four new supported tridentate Schiff base vanadium catalysts for the oxidative kinetic resolution of ethyl mandelate: a semi-soluble homopolymer catalyst (**2a'**), a semi-soluble copolymer catalyst (**2b'**), an insoluble cross-linked resin catalyst (**2c'**) and an insoluble silica supported catalyst (**3a**). The ligands and metalated catalysts have been characterized by a number of quantitative and qualitative techniques to ensure that the desired functionalities are present in the final supported catalysts. These catalysts are all active for oxidative kinetic resolution of ethyl mandelate, and all catalysts displayed roughly similar activity, with the supported catalysts somewhat slower than the parent homogeneous complex. The

mesoporous silica supported catalyst (**3a**) proved to be more selective than the other supported and homogeneous catalysts, suggesting that the nature of the supported catalyst (or linker) can influence the reaction selectivity. The insoluble catalysts (**2c'** and **3a**) were active for the kinetic resolution of ethyl mandelate and were recycled with similar yields after long reaction times for 4 cycles. If only these long time yields were reported, it could be suggested that the catalysts were recyclable with little loss in activity and equal selectivity. However, unlike most studies, recycle kinetics and catalyst decomposition were probed in this work, and they clearly demonstrated there was reduced catalyst activity in each run. Elemental analysis suggested cleavage of the imine functionality in the ligand and subsequent decomposition of the complex is a likely cause of the decreased catalyst activity upon recycle.

Experimental Section

General Remarks

3,5-Di-*tert*-butyl-2-hydroxybenzaldehyde (Aldrich), (*S*)-*tert*-leucinol (Aldrich), 3-isocyanatopropyltrimethoxysilane (Gelest), and vanadium(V) oxytriisopropoxide [VO(*O*-*i*-Pr)₃] (Aldrich) were used as received. 2,2'-Azo-bis(isobutyronitrile) (AIBN) (Aldrich) was dried under vacuum and stored in a nitrogen dry box. Styrene was distilled and stored in a nitrogen dry box. Divinylbenzene (Alfa Aesar) was treated with 20% sodium hydroxide to remove the stabilizer, washed with water, and dried over sodium sulfate prior to use. Dichloromethane and acetonitrile were dried over calcium hydride and distilled; chlorobenzene was dried with 4 Å molecular sieves and distilled under vacuum; acetone (BDH) was dried over anhydrous calcium sulfate and distilled. Toluene and tetrahydrofuran (THF) were used after purification and drying *via* a packed bed solvent system made of dual alumina columns.^[30]

Solution ¹H and ¹³C NMR spectroscopies were conducted on a Varian Mercury Vx 400 spectrometer. FT-IR spectroscopy was conducted on a Bruker Equinox 55 using disks made from solid catalyst samples dispersed in dry potassium bromide (KBr). The samples were analyzed using 1024 scans with a resolution of 4 cm⁻¹.

For single crystal X-ray diffraction, a suitable crystal of metalated-**2** was coated with Paratone N oil, suspended in a small fiber loop, and placed in a cooled nitrogen gas stream at 173 K on a Bruker D8 APEX II CCD sealed tube diffractometer with graphite monochromated MoK_α (0.71073 Å) radiation. Data were measured using a series of combinations of phi and omega scans with 10 s frame exposures and 0.5° frame widths. Data collection, indexing and initial cell refinements were carried out using APEX II software.^[31] Frame integration and final cell refinements were done using SAINT software.^[32] The final cell parameters were determined from least-squares refinement on 3626 reflections. The structure was solved using direct methods and difference Fourier techniques (SHELXTL, V6.12).^[33] Hydrogen

atoms were placed in their expected chemical positions using the HFIX command and were refined as riding atoms. All non-hydrogen atoms were refined anisotropically. Crystallographic data for the structure of metalated-2 has been deposited with the Cambridge Crystallographic Data Center as supplementary publication no. CCDC 695255. These data can be obtained free of charge from The Cambridge Crystallographic Data Centre via www.ccdc.cam.ac.uk/data_request/cif or on application to CCDC, 12 Union Road, Cambridge CB21EZ, UK (fax: (+44) 1223-336-033; email: deposit@ccdc.cam.ac.uk).

Nitrogen physisorption measurements were taken on a Micromeritics ASAP 2010 at 77 K. Prior to analysis, the as-synthesized SBA-15 sample was degassed with heating at 150 °C under vacuum overnight, and the functionalized SBA-15 sample was degassed with heating at 50 °C under vacuum overnight. Gas chromatography was used to monitor the reaction progress and was conducted on a Shimadzu GC 17 A equipped with a flame-ionization detector and a Chiraldex γ -TA column (length = 40 m, inner diameter = 0.25 mm, and film thickness = 0.25 μ m). The following temperature profile was used: heat to 90 °C, ramp to 140 °C at a rate of 6 °C min⁻¹, and hold for 11 min.

Synthesis of Schiff Base Ligand (1)

The homogeneous Schiff base ligand (**1**) was synthesized according to literature procedures (Scheme 2).^[11,34] 3,5-Di-*tert*-butyl-2-hydroxybenzaldehyde (4 g, 17 mmol) was dissolved in anhydrous methanol. Then, sodium sulfate (12.2 g) and (*S*)-*tert*-leucinol (2 g, 17 mmol) were added, and the mixture was stirred at room temperature for 4 h. The solution was filtered through Celite, the solvent was removed, and the product was dried under vacuum. The synthesis produced **1** as a yellow solid which was used without further purification; yield: 98%. ¹H NMR (400 MHz, CDCl₃): δ = 0.96 (s, 9H), 1.30 (s, 9H), 1.44 (s, 9H), 2.91 (dd, J = 9.48 and 2.72 Hz, 1H), 3.73 (m, 1H), 3.90 (m, 1H), 7.13 (d, J = 2.36 Hz, 1H), 7.39 (d, J = 2.32 Hz, 1H), 8.35 (s, 1H), 13.60 (s, 1H); ¹³C NMR (101 MHz, CDCl₃): δ = 27.4, 29.7, 31.7, 33.5, 34.4, 35.3, 62.8, 81.7, 117.9, 126.4, 127.4, 137.0, 140.4, 158.4, 167.4; anal. calcd. (%) for C₂₁H₃₅NO₂: C 75.63, H 10.58, N 4.20; found: C 75.39, H 10.64, N 4.24; accurate mass calcd.: 333.2668; found: 333.2656.

Synthesis of Styryl Functionalized Schiff Base Monomer (2) and Metalated-2

The styryl functionalized Schiff base monomer was prepared similarly to the homogeneous ligand **1** (Scheme 2). 3-*tert*-Butyl-2-hydroxy-5-(4'-vinylphenyl)benzaldehyde was synthesized according to published literature procedures.^[14,35] This styryl aldehyde (1.5 g, 5.35 mmol) was dissolved in anhydrous methanol. Then, sodium sulfate (4 g) and (*S*)-*tert*-leucinol (0.627 g, 5.35 mmol) were added, and the mixture was stirred at room temperature for 4 h. The solution was filtered through Celite, the solvent was removed, and the product was dried under vacuum. The synthesis produced **2** as a yellow solid which was used without further purification; yield: 98%. ¹H NMR (400 MHz, CDCl₃): δ = 0.98 (s, 9H), 1.48 (s, 9H), 2.95 (dd, J = 9.44 and 2.60 Hz, 1H), 3.76 (m, 1H), 3.96 (m, 1H), 5.25 (d, J = 10.88 Hz, 1H), 5.77 (d, J = 17.60 Hz, 1H), 6.74 (dd, J = 17.60 and 10.88 Hz, 1H),

7.37 (d, J = 2.12 Hz, 1H), 7.48 (m, 4H), 7.58 (d, J = 2.12 Hz, 1H), 8.42 (s, 1H), 13.94 (s, 1H); ¹³C NMR (101 MHz, CDCl₃): δ = 27.4, 29.6, 33.5, 35.3, 62.8, 81.6, 113.8, 118.8, 126.90, 126.95, 128.4, 128.7, 130.8, 136.2, 136.7, 138.1, 140.7, 160.4, 167.0; anal. calcd. (%) for C₂₅H₃₃NO₂: C 79.11, H 8.76, N 3.69; found: C 79.12, H 8.42, N 3.63; accurate mass calcd.: 379.2511; found: 379.2505.

For the crystal structure analysis, VO(O-*i*-Pr)₃ (0.09 g, 0.40 mmol) was added to a solution of **2** (0.17 g, 0.44 mmol) in methanol (5 mL). The reaction mixture was stirred for 4 h. The resulting dark brown solution was reduced to 2 mL and kept in the freezer to form brown colored crystals. Yield: 0.15 g. X-ray quality crystals were grown by recrystallization of metalated-2 from oxygenated ethanol.

Synthesis of Schiff Base Homopolymer Ligand (2a)

The styryl functionalized Schiff base monomer (**2**) was polymerized to form the homopolymer ligand (**2a**) (Scheme 3). In a typical preparation, monomer (0.25 g, 0.66 mmol) was added to a 15-mL pressure tube reaction vessel in a nitrogen dry box. Then, approximately 3 mL of dry, degassed chlorobenzene were added along with AIBN (11 mg, 0.067 mmol). The pressure tube was sealed and placed in an 80 °C oil bath and allowed to stir for 48 h. The reaction mixture was then cooled to room temperature and precipitated into cold hexanes. The precipitated polymer was filtered from the solution, washed with hexanes, and dried under vacuum to give **2a** as a yellow solid; yield: 76%; Mn: 5,330; PDI: 2.16.

Synthesis of Schiff Base Copolymer Ligand (2b)

The styryl functionalized Schiff base monomer (**2**) was copolymerized with styrene to form the copolymer ligand (**2b**) (Scheme 3). In a typical preparation, one equivalent of styryl Schiff base monomer (152 mg, 0.4 mmol) and four equivalents of styrene (167 mg, 1.6 mmol) were added to a 15-mL pressure tube reaction vessel in a nitrogen dry box. Then, approximately 3 mL of dry, degassed chlorobenzene were added along with AIBN (8.2 mg, 0.05 mmol). The pressure tube was sealed and placed in an 80 °C oil bath and allowed to stir for 48 h. The reaction mixture was then cooled to room temperature and precipitated into cold hexanes. The precipitated polymer was filtered from the solution, washed with hexanes, and dried under vacuum to give **2b** as a yellow solid; yield 63%; Mn: 8,439; PDI: 2.01.

Synthesis of Resin Supported Catalyst (2c')

The styryl functionalized Schiff base monomer (**2**) was cross-linked with divinylbenzene to form the resin **2c**. In a typical preparation, monomer **2** (0.50 g, 1.3 mmol) was dissolved in chlorobenzene (2.5 mL). Divinylbenzene (80%, mixture of isomers, 0.34 g, 2.6 mmol) was then added along with AIBN (0.04 g, 0.25 mmol), and the solution was purged with argon for 30 min. The solution was then stirred in an oil bath at 80 °C for 48 h. The cross-linked polymer **2c** obtained was filtered and washed with copious amounts of dichloromethane, toluene and methanol and subsequently dried under vacuum; yield: 0.81 g.

VO(O-*i*-Pr)₃ (172 mg, 0.70 mmol) was added to a suspension of resin **2c** (0.5 g) in ethanol and stirred in an oil bath at 60 °C for 24 h. The resulting metalated resin was filtered

and washed with copious amounts of ethanol and acetone to afford **2c'**; yield: 0.59 g; IR (KBr): $\nu=3017, 2955, 2914, 2865, 1620, 1544, 1436, 1269, 1173, 1068, 987, 896, 825 \text{ cm}^{-1}$; anal. found: C 75.44, H 7.29, N 2.14, V 5.3.

Synthesis of Hydroxy Functionalized Ligand (**3**)

3-*tert*-Butyl-5-chloromethyl-2-hydroxybenzaldehyde was synthesized according to published literature procedures.^[36] This compound was then converted to 3-*tert*-butyl-2-hydroxy-5-(hydroxymethyl)benzaldehyde.^[37] The 5-hydroxymethyl aldehyde (2.08 g, 10 mmol) was dissolved in anhydrous methanol. Then, sodium sulfate (6 g) and (*S*)-*tert*-leucinol (1.17 g, 10 mmol) were added, and the mixture was stirred at room temperature for 4 h (Scheme 2). The solution was filtered through Celite, the solvent was removed, and the product was dried. The product was purified *via* column chromatography (1:1 hexanes: ethyl acetate) and then recrystallized from methanol to produce **3** as a pure, pale yellow solid; yield: 79%; ¹H NMR (400 MHz, CDCl₃): $\delta=0.96$ (s, 9H), 1.42 (s, 9H), 1.55 (s, 2H), 2.92 (dd, $J=9.48$ and 2.76 Hz, 1H), 3.75 (m, 1H), 3.92 (m, 1H), 4.60 (d, $J=2.72$ Hz, 2H), 7.16 (d, $J=1.84$ Hz, 1H), 7.31 (d, $J=1.92$ Hz, 1H), 8.34 (s, 1H), 13.85 (s, 1H); ¹³C NMR (101 MHz, CDCl₃): $\delta=27.3, 29.6, 33.5, 35.1, 62.7, 65.6, 81.6, 118.5, 129.1, 129.3, 130.3, 138.0, 160.4, 166.8$; anal. calcd. (%) for C₁₈H₂₉NO₃: C 70.32, H 9.51, N 4.56; found: C 70.26, H 9.59, N 4.51; accurate mass calcd.: 307.2147; found: 307.2116.

Synthesis of SBA-15 Supported Catalyst (**3a**)

The SBA-15 silica support material was synthesized and calcined according to literature procedures, dried under vacuum at 200 °C for 3 h, and then stored in a nitrogen dry box prior to use.^[22,38] The hydroxy functionalized ligand (**3**) (0.25 g, 0.81 mmol) was first reacted with VO(O-*i*-Pr)₃ (188 mg, 0.77 mmol) by stirring the compounds in dry acetone under an oxygen blanket for 30 min. The acetone was removed under vacuum, and the metal complex was re-dissolved in dried tetrahydrofuran. Then, 3-isocyanatopropyltrimethoxysilane (183 mg, 0.89 mmol) was added to the solution in a nitrogen drybox along with triethylamine (90 mg, 0.89 mmol), and the solution was stirred at reflux conditions overnight (Scheme 5).^[39,40] The solvent was again removed, and the compound was dried under vacuum. The silane functionalized catalyst was dissolved in a small amount of toluene and added to a solution of calcined SBA-15 (0.45 g) in toluene in a nitrogen drybox. The slurry was stirred at reflux conditions overnight. The functionalized silica catalyst was filtered in the drybox and washed with copious amounts of toluene, hexanes, and acetone until each solvent ran clear. Catalyst **3a** was dried overnight under vacuum to give a light brown/maroon powder. The procedure yielded approximately 0.4 g of compound **3a**. Elemental analysis indicated a vanadium loading on the silica of 2 wt%.

Catalytic Reactions with *in situ* Metalation (Method 1)

Oxidative kinetic resolution reactions were performed *via* two methods. In the first method, the ligand was metalated *in situ* just prior to the reaction. The selected ligand (**1**, **2a**, or **2b**) (0.0825 mmol, 5.5 mol%) was added to the reaction

flask, followed by 3.5 mL of solvent. Once the ligand was completely dissolved, VO(O-*i*-Pr)₃ (17.5 μ L, 0.075 mmol, 5 mol%) was added to the flask. The catalyst mixture was allowed to stir under an oxygen blanket for 15 min. At the completion of this time, a solution of ethyl mandelate (270.3 mg, 1.5 mmol) and hexamethylbenzene (12.5 mg as an internal standard) in 4 mL of solvent was added to the reaction flask, and 100 μ L samples were taken periodically to monitor the extent of the reaction. An oxygen blanket was maintained in the flask throughout the course of the reaction.

Catalytic Reactions with Pre-Metalated Ligands (Method 2)

In the second method, the selected ligand was metalated and isolated prior to reaction. For the polymer catalysts **2a** and **2b**, the polymerized ligand first was dissolved in dry acetone. Then VO(O-*i*-Pr)₃ (0.9 equivalents) was added, and the solution was stirred under an oxygen blanket for 1½ hours. The solvent was removed. The metalated polymers were then dried under vacuum overnight. Cross-linked catalyst **2c'** was metalated as described above and always tested using Method 2. Silica catalyst **3a** was always tested with Method 2 and was never metalated after the ligand was anchored to the silica surface.

For the oxidative kinetic resolution, the selected metalated catalyst (**2a'**, **2b'**, **2c'** or **3a**) was added to the reaction flask at a 5 (or) 5.5 mol% vanadium loading (determined from elemental analysis) with 3.5 mL of solvent, and it was allowed to stir under an oxygen blanket for 15 min. At the completion of this time, a solution of ethyl mandelate (270.3 mg, 1.5 mmol) and hexamethylbenzene (12.5 mg as an internal standard) in 4 mL of solvent was added to the reaction flask, and 100 μ L samples were taken periodically to monitor the extent of the reaction. An oxygen blanket was maintained in the flask throughout the course of the reaction.

Acknowledgements

This work was supported by the DOE BES through Catalysis Science contract DE-FG02-03ER15459. We also thank Dr. Kenneth I. Hardcastle of Emory University for acquisition of the X-ray data.

References

- [1] G. M. Coppola, H. F. Schuster, *α -Hydroxy Acids in Enantioselective Synthesis* VCH, Weinheim, Germany, 1997.
- [2] J. B. Arterburn, *Tetrahedron* **2001**, 52, 9765.
- [3] M. J. Schultz, M. S. Sigman, *Tetrahedron* **2006**, 52, 8227.
- [4] R. Irie, T. Katsuki, *Chem. Rec.* **2004**, 4, 96.
- [5] D. E. J. E. Robinson, S. D. Bull, *Tetrahedron: Asymmetry* **2003**, 13, 1407.
- [6] W. Sun, H. Wang, C. Xia, J. Li, P. Zhao, *Angew. Chem. Int. Ed.* **2003**, 42, 1042.

- [7] Y. Nishibayashi, A. Yanauchi, G. Onodera, S. Uemura, *J. Org. Chem.* **2003**, *68*, 5875.
- [8] D. R. Jensen, J. S. Pugsley, M. S. Sigman, *J. Am. Chem. Soc.* **2001**, *123*, 7475.
- [9] E. M. Ferreira, B. M. Stoltz, *J. Am. Chem. Soc.* **2001**, *123*, 7725.
- [10] W. Sun, X. Wu, C. Xia, *Helv. Chim. Acta* **2007**, *90*, 623.
- [11] A. T. Radosevich, C. Musich, F. D. Toste, *J. Am. Chem. Soc.* **2005**, *127*, 1090.
- [12] S.-S. Weng, M.-W. Shen, J.-Q. Kao, Y. S. Munot, C.-T. Chen, *Proc. Natl. Acad. Sci. USA* **2006**, *103*, 3522.
- [13] C.-T. Chen, S. Bettigeri, S.-S. Weng, V. D. Pawar, Y.-H. Lin, C.-Y. Liu, W.-Z. Lee, *J. Org. Chem.* **2007**, *72*, 8175.
- [14] X. Zheng, C. W. Jones, M. Weck, *Chem. Eur. J.* **2006**, *12*, 576.
- [15] X. Zheng, C. W. Jones, M. Weck, *J. Am. Chem. Soc.* **2007**, *125*, 1105.
- [16] X. Zheng, C. W. Jones, M. Weck, *Adv. Synth. Catal.* **2008**, *350*, 255.
- [17] M. L. Kantam, T. Ramani, L. Chakrapani, B. M. Choudary, *J. Mol. Catal. A: Chem.* **2007**, *274*, 11.
- [18] R. I. Kureshy, I. Ahmad, K. Pathak, N.-U. H. Khan, S. H. R. Abdi, J. K. Prathap, R. V. Jasra, *Chirality* **2007**, *19*, 352.
- [19] J. Hartung, S. Drees, M. Greb, P. Schmidt, I. Svoboda, H. Fuess, A. Murso, D. Stalke, *Eur. J. Org. Chem.* **2003**, 2388.
- [20] M. R. Maurya, U. Kumar, I. Correia, P. Adao, J. C. Pessoa, *Eur. J. Inorg. Chem.* **2008**, 577.
- [21] R. J. H. Clark, *The Chemistry of Titanium and Vanadium*, Elsevier Publishing Company, Amsterdam, **1968**.
- [22] R. A. Shiels, C. W. Jones, *J. Mol. Catal. A: Chem.* **2007**, *261*, 160.
- [23] J. C. Hicks, C. W. Jones, *Langmuir* **2006**, *22*, 2676.
- [24] J. M. Richardson, C. W. Jones, *J. Catal.* **2007**, *251*, 80.
- [25] K. Miyazawa, S. Inagaki, *Chem. Commun.* **2000**, 2121.
- [26] C. S. Gill, K. Venkatasubbaiah, N. T. S. Phan, M. Weck, C. W. Jones, *Chem. Eur. J.* **2008**, *14*, 7306.
- [27] R. A. Sheldon, M. Wallau, I. Arends, U. Schuchardt, *Acc. Chem. Res.* **1998**, *31*, 485.
- [28] P. VanderVoort, K. Possemiers, E. F. Vansant, *J. Chem. Soc. Faraday Trans.* **1996**, *92*, 843.
- [29] M. Baltes, P. Van Der Voort, O. Collart, E. F. Vansant, *J. Por. Mater.* **1998**, *5*, 317.
- [30] A. B. Pangborn, M. A. Giardello, R. H. Grubbs, R. K. Rosen, F. J. Timmers, *Organometallics* **1996**, *15*, 1518.
- [31] *APEX II*, Bruker AXS, Inc., Analytical X-ray Systems, 5465 East Cheryl Parkway, Madison WI 53711–5373.
- [32] SAINT Version 6.45 A, Bruker AXS, Inc., Analytical X-ray Systems, 5465 East Cheryl Parkway, Madison WI 53711–5373.
- [33] SHELXTL V6.12, Bruker AXS, Inc., Analytical X-ray Systems, 5465 East Cheryl Parkway, Madison WI 53711–55373.
- [34] G. Liu, D. A. Cogan, J. A. Ellman, *J. Am. Chem. Soc.* **1997**, *119*, 9913.
- [35] H. Sellner, J. K. Karjalainen, D. Seebach, *Chem. Eur. J.* **2001**, *7*, 2873.
- [36] L. Canali, E. Cowan, H. Deleuze, C. L. Gibson, D. C. Sherrington, *J. Chem. Soc. Perkin Trans. 1* **2000**, 2055.
- [37] M. Holbach, X. Zheng, C. Burd, C. W. Jones, M. Weck, *J. Org. Chem.* **2006**, *71*, 2903.
- [38] D. Zhao, Q. Huo, J. Feng, B. F. Chmelka, G. D. Stucky, *J. Am. Chem. Soc.* **1998**, *120*, 6024.
- [39] N. Bellec, F. Lerouge, O. Jeannin, G. Cerveau, R. J. P. Corriu, D. Lorcy, *J. Organomet. Chem.* **2006**, *691*, 5774.
- [40] L. Chen, Y. Cui, G. Qian, M. Wang, *Dyes and Pigments* **2007**, *73*, 338.